

Mechanistic Comparison of the Cobalt-Substituted and Wild-Type Copper Amine Oxidase from *Hansenula polymorpha*

Stephen A. Mills,[‡] Yoshio Goto,^{‡,§} Qiaojuan Su,^{‡,||} Julie Plastino,^{‡,⊥} and Judith P. Klinman^{*,‡,⊙}

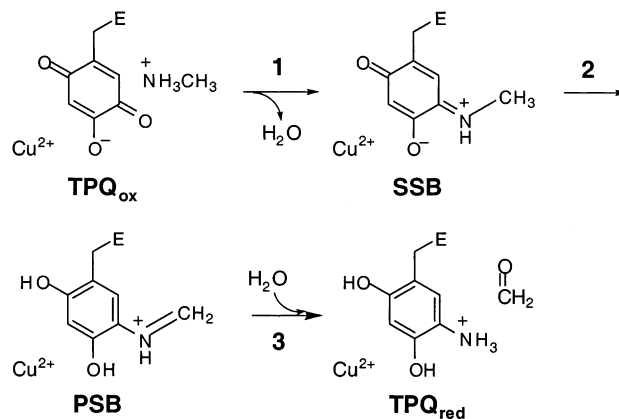
Department of Chemistry and Department of Molecular and Cell Biology, University of California, Berkeley, California 94720

Received January 29, 2002; Revised Manuscript Received June 13, 2002

ABSTRACT: A recent report by Mills and Klinman [Mills, S. A., and Klinman, J. P. (2000) *J. Am. Chem. Soc.* 122, 9897–9904] described the preparation and initial characterization of a cobalt-substituted form of the copper amine oxidase from *Hansenula polymorpha* (HPAO). This enzyme was found to be fully catalytically active at saturating substrate concentrations, but with a K_m for O_2 approximately 70-fold higher than that of the copper-containing, wild-type enzyme. Herein, we report a detailed analysis of the mechanism of catalysis for the wild-type and the cobalt-substituted forms of HPAO. Both forms of enzyme are concluded to utilize the same mechanism for oxygen reduction, involving initial, rate-limiting electron transfer from the reduced cofactor of the enzyme to prebound dioxygen. Superoxide formed in this manner is stabilized by the active site metal, facilitating the transfer of a second electron and two protons to form the product hydrogen peroxide. The elevated K_m for O_2 at the dioxygen binding site in Co-substituted HPAO, relative to that of wild-type HPAO, is proposed to be due to a change in the net charge at the adjacent metal site from +1 (cupric hydroxide) in wild-type enzyme to +2 (cobaltous H_2O) in cobalt-substituted HPAO.

The copper amine oxidases (CAOs),¹ a nearly ubiquitous class of enzymes among aerobic organisms, carry out the oxidative deamination of primary amines utilizing two cofactors: 2,4,5-trihydroxyphenylalanylquinone (TPQ) and a mononuclear Cu^{2+} ion. The oxidation of amines is carried out in two half-reactions with ping-pong kinetics. The reductive half-reaction, shown in Scheme 1, converts the resting form of the enzyme (TPQ_{ox}) to a substrate Schiff base (SSB) in the presence of primary amine substrates. Proton abstraction from the α -carbon of the amine substrate leads to formation of the product Schiff base (PSB). Hydrolysis of this PSB releases the aldehyde product and generates a reduced form of the enzyme with an aminoquinol form of TPQ (TPQ_{red}). In this manner, the reductive portion of the mechanism resembles an aminotransferase reaction.

Scheme 1: Mechanism of the Reductive Half-Reaction of HPAO^a



^a TPQ_{ox}, resting form of the enzyme; SSB, substrate Schiff base; PSB, product Schiff base; TPQ_{red}, reduced form of the enzyme.

* To whom correspondence should be addressed. Telephone: (510) 642-2668. Fax: (510) 643-6232. E-mail: klinman@socrates.berkeley.edu.

[‡] Department of Chemistry.

[§] Present address: ERATO Nanospace Project, Japan Science and Technology Corp., c/o National Museum of Emerging Science and Innovation, 2-41 Aomi, Koto-ku, Tokyo 135-0064, Japan.

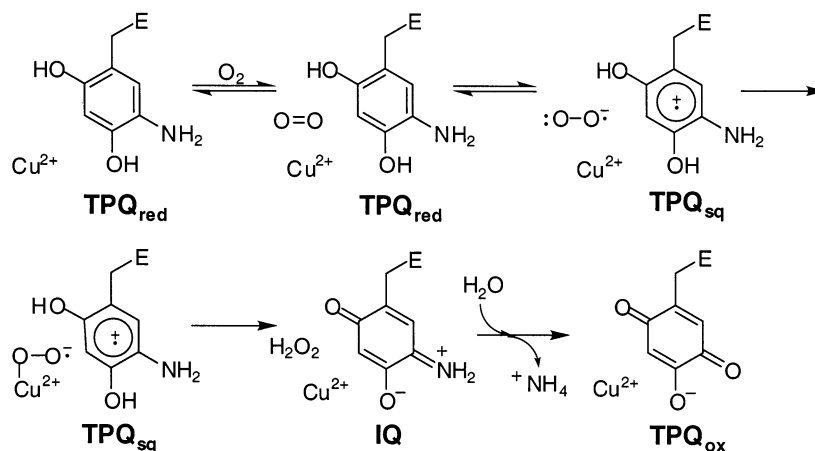
^{||} Present address: Abgenix, Inc., 6701 Kaiser Dr., M/S 11, Fremont, CA 94555.

[⊥] Present address: UMR 168/CNRS, Institut Curie, 26 rue d'Ulm, 75248 Paris cedex 05, France.

[⊙] Department of Molecular and Cell Biology.

¹ Abbreviations: CAO, copper amine oxidase; HPAO, copper amine oxidase from *H. polymorpha*; WT-HPAO, wild-type HPAO; Co-HPAO, Co^{2+} -substituted HPAO; BSAO, bovine serum amine oxidase; TPQ, 2,4,5-trihydroxyphenylalanylquinone; TPQ_{ox}, oxidized TPQ; TPQ_{sq}, semiquinone form of TPQ; TPQ_{red}, substrate-reduced form of TPQ; MeAm, methylamine; EPR, electron paramagnetic resonance; D_2O -, (k_{cat}/K_m), ratio of k_{cat}/K_m in H_2O to k_{cat}/K_m in D_2O .

In the oxidative half-reaction, TPQ_{red} reacts with dioxygen to form hydrogen peroxide and release ammonia. The mechanism of the oxidative half-reaction is less well understood and has been the subject of recent, intensive study (1–4). In particular, it has been difficult to isolate and characterize intermediates during conversion of TPQ_{red} to TPQ_{ox}. A primary point of controversy has been the path of electron transfer from TPQ_{red} to O_2 . Initially, it was proposed that the reduced form of the protein undergoes a catalytically functional, intramolecular electron transfer from TPQ_{red} to Cu^{2+} to form the semiquinone of TPQ (TPQ_{sq}) and Cu^+ ,

Scheme 2: Mechanism of the Oxidative Half-Reaction of BSAO As Proposed by Su and Klinman (2)^a

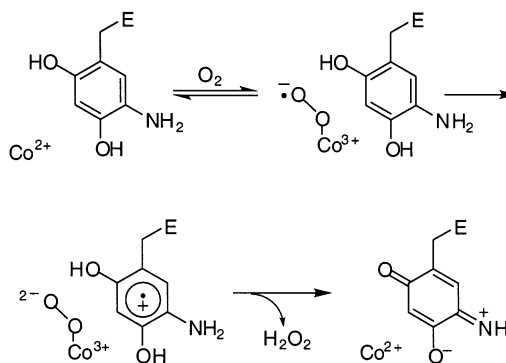
^a TPQ_{red}, reduced form of the enzyme; TPQ_{sq}, aminosemiquinone form of the enzyme; IQ, iminoquinone form of the enzyme; TPQ_{ox}, resting form of the enzyme.

with the latter being the site of reaction with O₂ (5). In subsequent detailed kinetic analyses of an amine oxidase from bovine serum (BSAO), Su and Klinman (2) proposed a prebinding of O₂ followed by a rate-limiting transfer of the first electron from TPQ_{red} directly to O₂ (Scheme 2). According to the mechanism in Scheme 2, the intermediate superoxide anion is stabilized by Cu²⁺ and undergoes a relatively rapid uptake of a second electron and two protons from TPQ_{sq}. The final step of the mechanism is hydrolysis of the iminoquinone species to regenerate TPQ_{ox}.

Along with kinetic studies, metal substitution has been pursued as a means of distinguishing the possible mechanisms for the oxidative half-reaction. An intramolecular transfer of an electron from TPQ_{red} to Cu²⁺, by its nature, requires a metal in the active site that can be reduced by one electron, whereas the mechanism in Scheme 2 does not have this requirement. Recently, Mills and Klinman (6) reported the preparation of a Co²⁺-substituted form of a copper amine oxidase from *Hansenula polymorpha* (HPAO) that is fully catalytically competent under conditions of O₂ saturation. As discussed by these authors, the highly unfavorable redox potential for Co²⁺ to Co⁺ (7) argues that Cu²⁺ need not undergo reduction during O₂ conversion to H₂O₂. However, since Co²⁺ is capable of interacting directly with oxygen, while Cu²⁺ is not, it was possible that Co-HPAO reduces oxygen by a mechanism different from that for the copper-containing WT-HPAO (Scheme 3). According to Scheme 3, reversible binding of O₂ to Co-HPAO leads to Co³⁺-O₂^{•-}, which might then be expected to undergo a rate-limiting one-electron transfer from TPQ_{red} to produce TPQ_{sq} and Co³⁺-O₂²⁻. An in-depth characterization of the copper and cobalt forms of HPAO was needed to conclude that both WT-HPAO and Co-HPAO proceed via the same mechanism. Here we present such a detailed study of both enzyme forms, demonstrating that, while differences exist between these forms, the overall mechanism for O₂ reduction appears unchanged.

EXPERIMENTAL PROCEDURES

Materials. All chemicals were purchased from commercial providers and used without further purification, except as noted. Oxygen was removed from nitrogen and argon

Scheme 3: Alternative Mechanism Proposed for Co-HPAO, Modified from ref 6^a

^a Oxygen interacts directly with Co²⁺, forming a Co³⁺-superoxide complex.

supplies by passing the gas stream through an alkaline solution of pyrogallol.

Enzyme Preparation. HPAO was expressed and purified as described by Plastino et al. (8) with the modifications described by Mills and Klinman (6). Protein concentrations were determined using the Bradford assay (Bio-Rad Laboratories) using bovine serum albumin as the protein standard. Co-HPAO was prepared according to the method of Mills and Klinman (6).

Phenylhydrazine derivatization was performed by adding a 5-fold molar excess of a freshly prepared phenylhydrazine·HCl solution to a sample of the protein. Spectra were recorded at 30 °C until the absorbance at 448 nm stopped increasing (typically, 15 min). An extinction coefficient of 40 500 M⁻¹ cm⁻¹ at 448 nm (9) and a subunit molecular weight of 75 700 (10) were used to determine the percentage of active TPQ cofactor in the protein.

Steady-State Kinetics. Initial velocity studies were carried out at 25 °C by following dioxygen consumption using a Clark electrode (Yellow-Springs 5300 oxygen monitor) as described by Hevel et al. (11). The pH dependencies of the kinetic parameters were measured with buffers as described by Hevel et al. For *k*_{cat}/*K*_m(O₂), methylamine was used as the amine substrate and was always at saturating concentrations. Initial velocity data were fitted to the Michaelis–Menten equation by nonlinear regression. Maximum velocity

values were converted to k_{cat} by correcting for the amount of TPQ present as determined by phenylhydrazine titration. For Co-HPAO, since the K_m for oxygen is high ($\sim 700 \mu\text{M}$ at pH 7), k_{cat} was determined by extrapolation of the Michaelis–Menten equation to saturating oxygen from data obtained up to $\sim 1 \text{ mM O}_2$. Maximum velocities and $\text{p}K_a$ s were determined by fitting the kinetic parameters to one of the equations shown below (12). Equation 1 is a three- $\text{p}K_a$ model, fitting a bell-shaped curve with an increase with two $\text{p}K_a$ s and a decrease with one $\text{p}K_a$. Equation 2 fits a bell-shaped curve with an increase and a decrease with one $\text{p}K_a$ each. Equation 3 fits an increase with two $\text{p}K_a$ s. Equation 4 fits an increase with one $\text{p}K_a$. The parameter x can be either k_{cat}/K_m or k_{cat} .

$$\log(x) = \log(x)_{\text{max}} - \log(1 + 10^{\text{p}K_a1 - \text{pH}} + 10^{\text{p}K_a1 + \text{p}K_a2 - 2\text{pH}} + 10^{\text{pH} - \text{p}K_a3}) \quad (1)$$

$$\log(x) = \log(x)_{\text{max}} - \log(1 + 10^{\text{p}K_a1 - \text{pH}} + 10^{\text{pH} - \text{p}K_a2}) \quad (2)$$

$$\log(x) = \log(x)_{\text{max}} - \log(1 + 10^{\text{p}K_a1 - \text{pH}} + 10^{\text{p}K_a1 + \text{p}K_a2 - 2\text{pH}}) \quad (3)$$

$$\log(x) = \log(x)_{\text{max}} - \log(1 + 10^{\text{p}K_a - \text{pH}}) \quad (4)$$

Titration of the Reduced Cofactor as a Function of pH. As described previously (2), a stock solution of HPAO (50–100 μM) was introduced into a Slide-A-Lyzer cassette (10 kDa cutoff, Pierce) and dialyzed overnight at 4 °C in buffer at the desired pH. The same buffers were used that were used for the kinetic assays described above. The sample was removed from the cassette, and the precipitated protein was removed by centrifugation prior to use. An aliquot (300 μL) of the solution was transferred to a UV-vis cuvette fitted with a ground-glass joint and sealed with a septum. The oxygen was removed from the solution by passing oxygen free Ar over the sample for 45 min. A spectrum was taken at 25 °C (oxidized form of the enzyme). Deoxygenated MeAm was added to the solution, via a gastight syringe, to a final concentration of 700 μM , and a second spectrum was taken (reduced form of the enzyme). The change in absorbance at 310 and 500 nm was measured as a function of pH and fitted to eq 5, where y is the ratio of absorbance at 310 and 500 nm.

$$y = \frac{y_{\text{max}}}{1 + 10^{\text{p}K_a - \text{pH}}} + \frac{y_{\text{min}}}{1 + 10^{\text{pH} - \text{p}K_a}} \quad (5)$$

Solvent Isotope Effects on $k_{\text{cat}}/K_m(\text{O}_2)$. Initial rates for the oxidation of MeAm by WT-HPAO were measured in D_2O using the oxygen electrode as described above. The pH meter electrode was soaked in D_2O before use, and 0.4 was added to pH readings to give pD values (13). The oxygen electrode probe was stored in D_2O between assays. In the case of Co-HPAO, the solvent isotope effect is the result of a single, appropriately chosen pD; in this instance, the propagated error from the D_2O measurement on the isotope effect reflects the standard error of the curve fitting.

Viscosity Effect. The viscosity effect on $k_{\text{cat}}/K_m(\text{O}_2)$ was measured on a Clark electrode at pH 7.8 (WT-HPAO) and pH 7.4 (Co-HPAO) in 100 mM potassium phosphate buffer

with 10 mM MeAm and an ionic strength of 300 mM at 25 °C. Glucose or sucrose was added to the buffer to give the relative viscosities indicated prior to adjusting the pH. The relative viscosity of the glucose solutions was measured against buffer with no glucose using an Ostwald viscometer immersed in a water bath at 25 °C. The reported relative viscosity is an average of five determinations at each glucose concentration. Data were fitted to eq 6 (14), where k_{cat}/K_m° is k_{cat}/K_m in the absence of viscosogen and η/η° is the relative viscosity of the solution. The slope of the line, S , reflects the degree of viscosity dependence (14).

$$\frac{k_{\text{cat}}/K_m}{k_{\text{cat}}/K_m^\circ} = S\left(\frac{\eta}{\eta^\circ} - 1\right) + 1 \quad (6)$$

^{18}O Isotope Effects. ^{18}O kinetic isotope effects were measured as previously described (2, 15). Reactions were performed at 25 °C in oxygen-saturated buffer containing 100 mM potassium phosphate (pH 7.8, 300 mM ionic strength) and 6 mM MeAm (WT-HPAO) or 3 mM MeAm (Co-HPAO). The reaction was coupled with horseradish peroxidase (10 nM) using potassium ferrocyanide (3 mM) as the substrate to convert H_2O_2 to H_2O . Guaiacol was used in place of ferrocyanide in the previous work with BSAO (2), but was found to be inhibitory toward HPAO (data not shown).

Turnover Species. The turnover species for WT-HPAO were observed by adding enzyme to buffer containing 100 mM potassium phosphate buffer at pH 7.1, an ionic strength of 300 mM, and 25 °C, giving a final enzyme concentration of 27 μM . This was the initial spectrum. Methylamine was added to a final concentration of 0.5 mM, and spectra were taken at 15 s intervals for at least several minutes or until the spectra stopped changing. The difference spectra were generated by subtracting the initial spectrum from the spectrum at a given time.

The turnover species for Co-HPAO were observed in the same way as they were for WT-HPAO except that the buffer was saturated with oxygen prior to addition of substrate. The final enzyme concentration was 33 μM , and the final methylamine concentration was 2.2 mM.

RESULTS

pH Profiles for $k_{\text{cat}}/K_m(\text{O}_2)$. The effect of pH on $k_{\text{cat}}/K_m(\text{O}_2)$ for WT-HPAO is shown in Figure 1. There is an increase in $k_{\text{cat}}/K_m(\text{O}_2)$ with increasing pH, reaching a maximum of $(1.04 \pm 0.17) \times 10^6 \text{ M}^{-1} \text{ s}^{-1}$ around pH 8.5 and showing $\text{p}K_a$ s of 6.8 ± 0.1 and 7.9 ± 0.1 . Since no effect of solvent deuteration was observed with BSAO (2), a detailed analysis of the effect of solvent deuteration was not performed on HPAO. However, $k_{\text{cat}}/K_m(\text{O}_2)$ was evaluated in D_2O at pD 8.6 and 9.3 (in the plateau region of the curve). The average value of $k_{\text{cat}}/K_m(\text{O}_2)$ at these two pDs was not significantly different from the average value of $k_{\text{cat}}/K_m(\text{O}_2)$ in H_2O measured at pH 7.9 and 8.9 [$^{18}\text{O}(k_{\text{cat}}/K_m) = 1.2 \pm 0.3$].

The effect of pH on $k_{\text{cat}}/K_m(\text{O}_2)$ for Co-HPAO is also shown in Figure 1. There is an increase in $k_{\text{cat}}/K_m(\text{O}_2)$ as the pH increases from 6 to 7.5, with a $\text{p}K_a$ of 6.7 ± 0.1 . As the pH is increased above pH 7.5, $k_{\text{cat}}/K_m(\text{O}_2)$ remains constant

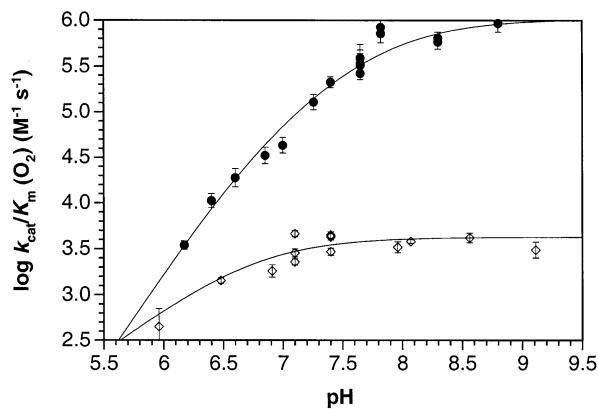


FIGURE 1: $\log[k_{\text{cat}}/K_m(\text{O}_2)]$ vs pH for WT-HPAO and Co-HPAO. Data for WT-HPAO (●) are fitted to a two- pK_a model, eq 3 (Experimental Procedures): maximum = $(1.04 \pm 0.17) \times 10^6 \text{ M}^{-1} \text{ s}^{-1}$, $\text{pK}_{a1} = 6.8 \pm 0.1$, and $\text{pK}_{a2} = 7.9 \pm 0.1$ (21). Data for Co-HPAO (◇) are fitted to a single- pK_a model, eq 4 (Experimental Procedures): maximum = $(4.23 \pm 0.16) \times 10^3 \text{ M}^{-1} \text{ s}^{-1}$ and $\text{pK}_a = 6.7 \pm 0.1$.

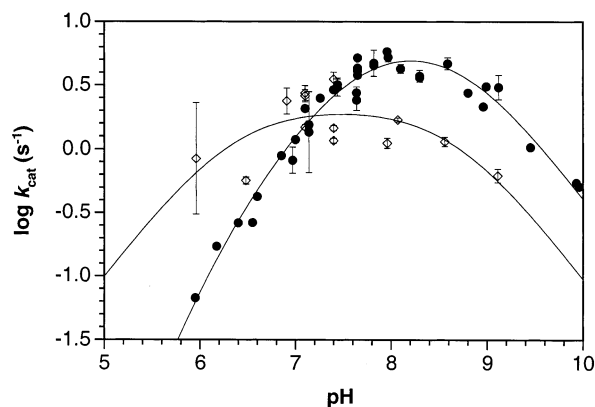


FIGURE 2: $\log k_{\text{cat}}$ vs pH for WT-HPAO and Co-HPAO. WT-HPAO data (●) are fitted to a three- pK_a model, eq 1 (Experimental Procedures): maximum = $7.8 \pm 1.2 \text{ s}^{-1}$, $\text{pK}_{a1} = 6.1 \pm 0.2$, $\text{pK}_{a2} = 7.7 \pm 0.1$, and $\text{pK}_{a3} = 8.7 \pm 0.1$ (11, 21). Co-HPAO data (◇) are fitted to a two- pK_a model, eq 2 (Experimental Procedures): maximum = $2.1 \pm 0.5 \text{ s}^{-1}$, $\text{pK}_{a1} = 6.3 \pm 0.3$, and $\text{pK}_{a2} = 8.7 \pm 0.3$.

at $(4.23 \pm 0.16) \times 10^3 \text{ M}^{-1} \text{ s}^{-1}$. Solvent deuteration had no significant effect on $k_{\text{cat}}/K_m(\text{O}_2)$ at pD 8.5 [$^2\text{D}_0(k_{\text{cat}}/K_m) = 1.4 \pm 0.3$].

Titration of TPQ_{red} . Difference UV–vis spectral titration of the anaerobic, substrate-reduced form of the cofactor in WT-HPAO was characterized. All spectra were normalized at 500 nm, where only the oxidized form of the enzyme (TPQ_{ox}) absorbs. Upon reduction, there is a loss of absorbance at 480 nm due to a loss of TPQ_{ox} and an appearance of absorbance at 310 nm due to the formation of the reduced form of the cofactor (TPQ_{red}). The change in absorbance at 310 nm increases with pH. The change in absorbance at 480 nm is not pH sensitive; however, with increasing pH absorbance due to the semiquinone form of TPQ (TPQ_{sq}) appears at 464 nm (5). The absolute value of the ratio of the increase in absorbance at 310 nm to the decrease in absorbance at 500 nm provides an estimate of the pK_a of the reduced cofactor (7.2 ± 0.2).

pH Profiles for k_{cat} . The effect of pH on k_{cat} for WT-HPAO is shown in Figure 2. The response of k_{cat} to pH is bell-shaped, increasing from pH 6 to 8 and reaching a maximum

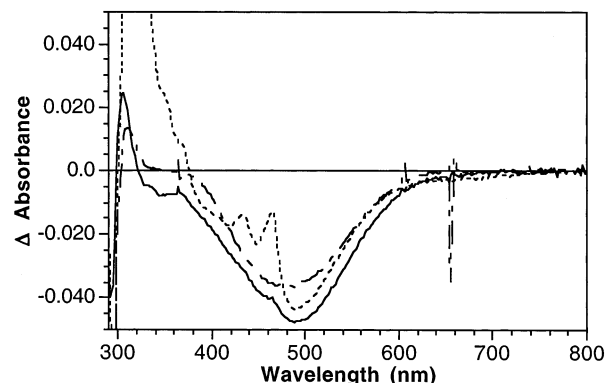


FIGURE 3: Species that accumulate during turnover for WT-HPAO and Co-HPAO. A spectrum was taken prior to addition of 2.5 mM MeAm. Subsequent spectra were taken at 15 s intervals after substrate addition and subtracted from the initial spectrum. No significant change is seen in the spectra after 15 s. The spectra shown were taken 60 s after substrate addition to WT-HPAO at pH 7.1 (—), WT-HPAO at pH 9.5 (···), and Co-HPAO at pH 7.1 (---). In all cases, the change in absorbance at 480 nm corresponds to complete bleaching of the oxidized cofactor. Conditions: 100 mM KPi , pH 7.1, $\mu = 300 \text{ mM}$, and 25°C or 100 mM KHCO_3 , pH 9.5, and $\mu = 300 \text{ mM}$, where $[\text{WT-HPAO}] = 34 \mu\text{M}$, 66% TPQ, and $[\text{Co-HPAO}] = 33 \mu\text{M}$, 57% TPQ.

value of $7.8 \pm 1.2 \text{ s}^{-1}$ with pK_a s of 6.1 ± 0.2 and 7.7 ± 0.1 . The value of k_{cat} decreases as the pH is increased from pH 8 with a pK_a of 8.7 ± 0.1 . A similar response of k_{cat} to pH was reported previously (11), but with only two pK_a s in the profile. The data at that time did not indicate more than two pK_a s; however, with the larger amount of data available, a third pK_a is required to fit the points at low pH.

The response of k_{cat} for Co-HPAO to pH is bell-shaped, increasing from pH 6 to 7.5 to a maximum value of $2.1 \pm 0.5 \text{ s}^{-1}$ with a pK_a of 6.3 ± 0.3 (Figure 2). As the pH is increased further, k_{cat} decreases with a pK_a of 8.7 ± 0.3 . Although the low pK_a is not fully characterized, it is clear that the pK_a at 7.7, seen with WT-HPAO, is absent.

Loss of TPQ_{ox} during Catalytic Turnover. Shown in Figure 3 are the difference spectra of WT-HPAO after aerobic substrate addition to enzyme at pH 7.1 and 9.5. In both cases, there is an immediate loss of absorbance at 480 nm due to a loss of TPQ_{ox} . There is a concomitant increase in absorbance at 310 nm due to TPQ_{red} . At pH 9.5, the absorbance at 310 nm is more pronounced due to the extinction coefficient of the deprotonated TPQ_{red} being larger than that of the protonated form (16). Also seen at pH 9.5 is marked absorbance due to TPQ_{sq} (peak at 464 nm), similar to what is observed anaerobically (see above). Formation of TPQ_{sq} under these conditions is attributed to noncatalytic transfer of an electron from TPQ_{red} to Cu^{2+} to form TPQ_{sq} and Cu^+ .

Also shown in Figure 3 is the difference spectrum of Co-HPAO upon aerobic addition of substrate at pH 7.1. As with the wild type, there is a decrease in absorbance at 480 nm and a concomitant increase at 310 nm, due to reduction of TPQ_{ox} to TPQ_{red} . No absorbance due to TPQ_{sq} has been observed, consistent with the much more negative reduction potential for Co^{2+} (7).

Comparative $k_{\text{cat}}/K_m(\text{MeAm})$ Values. At pH 7.1, k_{cat}/K_m (MeAm) for WT-HPAO is $(3.77 \pm 0.11) \times 10^4 \text{ M}^{-1} \text{ s}^{-1}$. The substrate isotope effects on k_{cat} and k_{cat}/K_m are 1.20 ± 0.03 and 5.41 ± 0.4 , respectively (11). At the same pH, $k_{\text{cat}}/$

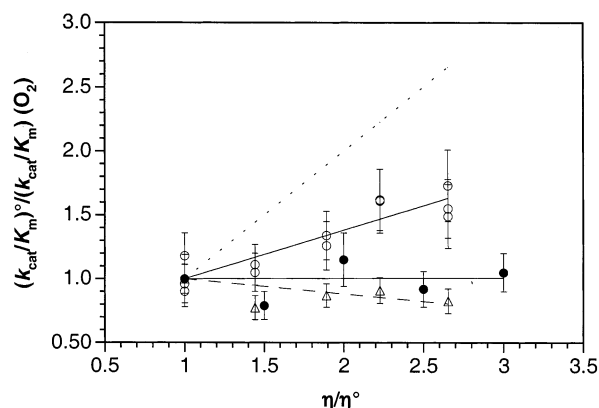


FIGURE 4: Viscosity effect on $k_{\text{cat}}/K_m(\text{O}_2)$ for WT-HPAO and Co-HPAO. $k_{\text{cat}}/K_m(\text{O}_2)$ for WT-HPAO with glucose as the viscosogen (○) and with sucrose as the viscosogen (●). $k_{\text{cat}}/K_m(\text{O}_2)$ for Co-HPAO (△) with glucose as the viscosogen. Data are fitted to eq 6 (Experimental Procedures). The dotted line represents 100% diffusion control.

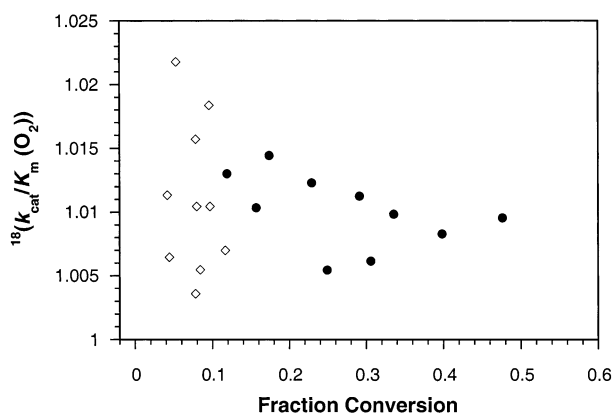


FIGURE 5: ^{18}O kinetic isotope effect for WT-HPAO and Co-HPAO. The average value for WT-HPAO (●) = 1.0101 ± 0.0029 . The average value for Co-HPAO (△) = 1.0101 ± 0.0052 . A more complete data set could not be obtained for Co-HPAO due to enzyme inactivation during the assay.

$K_m(\text{MeAm})$ for Co-HPAO is $(1.58 \pm 0.63) \times 10^4 \text{ M}^{-1} \text{ s}^{-1}$. The substrate isotope effects for Co-HPAO on k_{cat} and k_{cat}/K_m are 1.52 ± 0.16 and 4.36 ± 1.8 , respectively.

Viscosity Effect on $k_{\text{cat}}/K_m(\text{O}_2)$. The effect of viscosogen on $k_{\text{cat}}/K_m(\text{O}_2)$ for WT-HPAO is shown in Figure 4. As can be seen, $k_{\text{cat}}/K_m(\text{O}_2)$ decreases slightly when glucose is used as the viscosogen. However, this appears to be specific to WT-HPAO and glucose, since the use of sucrose eliminates the reduction in rate seen with glucose.

Similarly, the use of glucose with Co-HPAO leads to practically unchanged values for $k_{\text{cat}}/K_m(\text{O}_2)$. The slightly inhibitory effect of glucose on WT-HPAO is tentatively attributed to a reaction between the reducing sugar, glucose, and the active site Cu^{2+} of WT-HPAO.

^{18}O Isotope Effect on $k_{\text{cat}}/K_m(\text{O}_2)$. The ^{18}O isotope effects on $k_{\text{cat}}/K_m(\text{O}_2)$ for WT- and Co-HPAO at pH 7.8 are shown in Figure 5. The data for WT-HPAO were collected between 10 and 50% substrate conversion, yielding an isotope effect of 1.0101 ± 0.0029 . For Co-HPAO, it was not possible to obtain data for fractional conversions of $>10\%$ due to enzyme instability. The data indicate a similar average isotope effect, but with greater scatter (1.0101 ± 0.0052), due to the smaller enrichment of ^{18}O in unreacted O_2 at low fractional conversions (15). The instability of Co-HPAO is

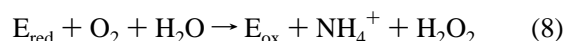
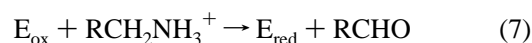
Table 1: Summary of Kinetic Parameters for $k_{\text{cat}}/K_m(\text{O}_2)$

	WT-HPAO	Co-HPAO
maximum ($\text{M}^{-1} \text{ s}^{-1}$)	$(1.04 \pm 0.17) \times 10^6$	$(4.23 \pm 0.16) \times 10^3$
$\text{pK}_{\text{a}1}$	6.8 ± 0.1	6.7 ± 0.1
$\text{pK}_{\text{a}2}$	7.9 ± 0.1	—
$k_{\text{H}_2\text{O}}/k_{\text{D}_2\text{O}}$	1.2 ± 0.3	1.4 ± 0.3

likely due to oxidation of Co^{2+} to Co^{3+} by hydrogen peroxide formed in the active site during catalysis.

DISCUSSION

Effects on $k_{\text{cat}}/K_m(\text{MeAm})$. The reaction catalyzed by the copper amine oxidases can be broken down into two half-reactions involving substrate oxidation [$k_{\text{cat}}/K_m(\text{MeAm})$, reductive half-reaction, eq 7] and oxygen reduction [$k_{\text{cat}}/K_m(\text{O}_2)$, oxidative half-reaction, eq 8].



As a control for the properties of the oxidative half-reaction, the properties of the reductive half-reaction of Co-HPAO were studied at a single pH for comparison to the properties of WT-HPAO. These studies showed that Co^{2+} slows MeAm oxidation by a factor of ca. 2–3. The substrate isotope effect of 4.4 (compared to 5.4 for WT-HPAO) indicates that C–H abstraction dominates $k_{\text{cat}}/K_m(\text{MeAm})$ for both enzyme forms. Clearly, substitution of Cu^{2+} with Co^{2+} has only subtle effects on the first half-reaction. Similar effects have also been seen with CAOs from other sources (17, 18).

Effects on $k_{\text{cat}}/K_m(\text{O}_2)$. In the initial study of Co-HPAO, k_{cat} for Co-HPAO was reported to be the same as for the wild-type enzyme at pH 7.1 but $k_{\text{cat}}/K_m(\text{O}_2)$ was reduced almost 2 orders of magnitude (6). In this study, we have performed full rate versus pH studies for a more complete comparison of Co-HPAO and WT-HPAO. The data shown in Figure 1 are summarized in Table 1. Whereas the overall shapes of the pH profiles look similar for WT-HPAO and Co-HPAO (Figure 1), the fitted data indicate one less pK_{a} for the cobalt enzyme (Table 1). In an earlier study of BSAO, two pK_{a} s were reported for the pH dependence of $k_{\text{cat}}/K_m(\text{O}_2)$. From the titration of the reduced cofactor by UV–vis spectroscopy and by EPR, one of the two kinetic pK_{a} s could be assigned to the ionization of the reduced cofactor. The remaining kinetic pK_{a} was ascribed to the ionization of a copper-bound water molecule, although no direct data were available at the time to support this assignment.

In the study presented here, the UV–vis approach was taken to assign the pK_{a} of TPQ_{red} in WT-HPAO, leading to an estimate of 7.2 ± 0.2 for the conversion of the protonated aminoquinol of TPQ_{red} to its neutral form. The value of this pK_{a} lies between the two values determined from kinetic studies, precluding assignment of the two kinetically determined values. However, comparison of the kinetic data for the wild-type and cobalt enzymes shows that the pK_{a} of 7.9 is lost following metal substitution. A similar loss appears in the analysis of k_{cat} (Figure 2 and Table 2), where the pK_{a} of 7.7 can no longer be detected upon substitution of copper with cobalt. Solution studies of aquo-copper versus aquo-cobalt indicate an increase in pK_{a} from ca. 8.0 to 9.7 (19).

Table 2: Summary of Kinetic Parameters for k_{cat}

	WT-HPAO	Co-HPAO
maximum (s^{-1})	7.8 ± 1.2	2.1 ± 0.5
$\text{p}K_{\text{a}1}$	6.1 ± 0.2	6.3 ± 0.3
$\text{p}K_{\text{a}2}$	7.7 ± 0.1	—
$\text{p}K_{\text{a}3}$	8.7 ± 0.1	8.7 ± 0.3

It is most reasonable to assume that the $\text{p}K_{\text{a}}$ for the metal-bound water molecule in WT-HPAO is 7.9 and that the $\text{p}K_{\text{a}}$ for the cobalt-bound water molecule in Co-HPAO is shifted to outside the experimental pH range. Measurement of $k_{\text{cat}}/K_{\text{m}}(\text{O}_2)$ above pH 9.2 was precluded by the greatly reduced activity of Co-HPAO at high pH. We, therefore, conclude that the two kinetic $\text{p}K_{\text{a}}$ s for WT-HPAO reflect the ionization of TPQ_{red} (6.8) and copper-bound water (7.9).

The mechanistic findings of these pH-dependent studies on $k_{\text{cat}}/K_{\text{m}}(\text{O}_2)$ are 3-fold. First, as in earlier studies with native BSAO, it can be concluded that the neutral form of TPQ_{red} is the cofactor form responsible for electron transfer to dioxygen. Second, the replacement of copper with cobalt in HPAO has no detectable effect on the kinetically determined $\text{p}K_{\text{a}}$ of the reduced cofactor. As was seen with BSAO, this $\text{p}K_{\text{a}}$ is elevated relative to a model compound of the free cofactor, which exhibits a $\text{p}K_{\text{a}}$ of 5.9. This $\text{p}K_{\text{a}}$ perturbation can be attributed to electrostatic stabilization of the protonated amino form of TPQ_{red} by a neighboring carboxylate (Asp 319). Third, dioxygen reactivity in WT-HPAO occurs most efficiently from an enzyme form containing hydroxide ion bound to the metal. In the case of Co-HPAO, we conclude that the cobalt-bound water is not ionized, indicating that the reaction of the free enzyme with O_2 can occur from an un-ionized form of the metal–water complex, but at a much reduced rate.

Effects on k_{cat} . In contrast with the dramatic effect on $k_{\text{cat}}/K_{\text{m}}(\text{O}_2)$, substitution of copper by cobalt has a relatively small effect on k_{cat} at all pH values studied (Figure 2). In the previously reported comparison of k_{cat} for WT- and Co-HPAO (6), we had chosen (fortuitously) the one pH (7.0) where the rates are identical. A more meaningful comparison is possible with the determination of full rate versus pH profiles. At the point of the maximum rate for both WT-HPAO and Co-HPAO, Co-HPAO is now seen to be 3–4-fold slower than WT-HPAO.

The two acidic $\text{p}K_{\text{a}}$ values in the k_{cat} profile with WT-HPAO are similar to those seen on $k_{\text{cat}}/K_{\text{m}}(\text{O}_2)$. While these are kinetic $\text{p}K_{\text{a}}$ values, and may be shifted from thermodynamic values, it is still useful to contrast the values with those seen on $k_{\text{cat}}/K_{\text{m}}(\text{O}_2)$. Importantly, the appearance of the $\text{p}K_{\text{a}}$ assigned to copper-bound water (7.7) in k_{cat} has mechanistic significance, implicating the presence of metal-bound water in the active site when O_2 is saturating. As discussed below, this observation, together with other arguments, allows us to rule out a mechanism in which an obligatory loss of metal-bound water prior to O_2 binding is the origin of the greatly diminished rate of $k_{\text{cat}}/K_{\text{m}}(\text{O}_2)$ with Co-HPAO.

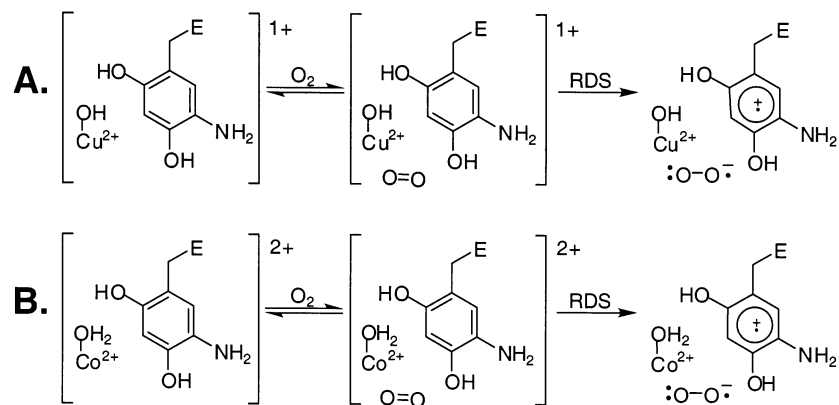
Mechanistic Comparison of Co-HPAO to WT-HPAO. The effect of cobalt substitution on $k_{\text{cat}}/K_{\text{m}}(\text{O}_2)$ (Figure 1 and Table 1) contrasts with that for k_{cat} , where the pH profiles are shifted, but plateau values are almost identical for WT-HPAO and Co-HPAO (Figure 2 and Table 2). This dif-

ferential impact of metal substitution on $k_{\text{cat}}/K_{\text{m}}(\text{O}_2)$ versus k_{cat} could reflect the fact that very different steps are rate-limiting for the two parameters. However, examination of the species that accumulate under turnover conditions with saturating amine and O_2 (Figure 3) indicates that TPQ_{red} is the dominant cofactor form with both WT-HPAO and Co-HPAO. As shown in eq 8, TPQ_{red} is the form of enzyme that determines $k_{\text{cat}}/K_{\text{m}}(\text{O}_2)$. Thus, the data in Figure 3 support a similar rate-limiting step for k_{cat} and $k_{\text{cat}}/K_{\text{m}}(\text{O}_2)$ with both WT-HPAO and Co-HPAO.

Both enzyme forms show measurable ^{18}O kinetic isotope effects that are within experimental error of one another (Figure 5) and similar to a value reported earlier for BSAO [1.0097 ± 0.0010 (2)]. These ^{18}O isotope effects are consistent with a similar rate-limiting electron transfer from TPQ_{red} to O_2 with both Co-HPAO and WT-HPAO. The magnitude of these isotope effects implicates a mechanism for $k_{\text{cat}}/K_{\text{m}}(\text{O}_2)$ in which O_2 , prebound to the active site, undergoes a rate-limiting one-electron transfer from the neutral aminoquinol form of the cofactor ($\text{p}K_{\text{a}} = 7.2$). In the event that a $\text{Co}^{3+}\text{O}_2^{\bullet-}$ mechanism were operating, the ^{18}O kinetic isotope effect would be expected to reflect the formation of $\text{Co}^{3+}\text{O}_2^{2-}$ from free O_2 . However, it appears extremely unlikely that disparate chemical mechanisms for WT- and Co-HPAO could produce *both* similar k_{cat} values and kinetic isotope effects that are within experimental error of one another. Analogous results (both the species that accumulate during turnover and the ^{18}O isotope effects) have been obtained with native BSAO, where it was concluded that electron transfer from a reduced cofactor to O_2 significantly limits catalysis at both low and saturating concentrations of O_2 (2).

Since the initial report of a kinetic ^{18}O isotope effect of 1.01 for outer sphere electron transfer to O_2 from TPQ_{red} in BSAO, several other systems have been characterized that catalyze similar outer sphere electron transfer reactions. These include tyrosine hydroxylase in which the electron donor is a reduced pterin (20) and glucose oxidase in which the electron donor is a reduced flavin (14). In these two systems, the magnitudes of the measured ^{18}O isotope effects are larger than that seen for BSAO (2) and HPAO (this study), raising the question of the origin of the reduced isotope effect seen with the CAOs. One possibility was that the superoxide ion produced upon TPQ_{red} oxidation was undergoing some stabilization by the neighboring $\text{Cu}(\text{II})$. This could occur at the empty, equatorial site for WT-HPAO, which may or may not be present in Co-HPAO (see the discussion below). In actuality, application of Marcus theory to single, outer sphere electron transfer reactions to O_2 predicts a wide range of ^{18}O kinetic isotope effects, which vary as a function of reaction driving force (ΔG°) and the size of the reorganization term (λ) (J. P. Roth and J. P. Klinman, unpublished results). The potential observation of a range of ^{18}O isotope effects in a single enzyme system is currently under investigation using glucose oxidase, where it is possible to vary both λ and ΔG° by varying the cofactor structure and reaction conditions.

With the implication of the same rate-limiting steps, what is the cause of the diminished rate of $k_{\text{cat}}/K_{\text{m}}(\text{O}_2)$ following copper substitution with cobalt, and what role does metal–water ionization play in the wild-type enzyme? In previous discussions of the mechanism of the oxidative half-reaction

Scheme 4: Proposed Mechanism of the Oxidative Half-Reaction of HPAO^a

^a On the basis of the X-ray structure of the substrate-reduced *E. coli* CAO (4), a single water molecule is shown bound to the active site copper atom. (A) From the studies herein, WT-HPAO is expected to react in the copper-bound hydroxide state. (B) From the shifts in pK_a for Co-HPAO, this enzyme is proposed to react from the cobalt-bound water state.

of the CAOs, it has been pointed out that oxidation involves the net loss of two electrons and two protons from TPQ_{red} (2). Ionization of metal-bound water to hydroxide ion may be expected to generate a base for proton abstraction from the cofactor in the course of its oxidation. Importantly, rate limitation by proton transfer can be ruled out by the lack of a significant solvent deuterium isotope effect on $k_{\text{cat}}/K_m(\text{O}_2)$ for both WT-HPAO and Co-HPAO (Table 1). Similar results were observed with native BSAO where it was concluded that proton transfer is fast relative to an initial, rate-limiting electron transfer step. From these studies, it is particularly surprising that the greatly reduced value of $k_{\text{cat}}/K_m(\text{O}_2)$, together with the elevated pK_a for cobalt-bound water, does not manifest itself in a rate-limiting proton transfer step.

It was also possible that binding of O_2 to the enzyme had become partially rate-limiting for Co-HPAO, introducing a kinetic barrier that is not present in WT-HPAO and slowing the observed rate of $k_{\text{cat}}/K_m(\text{O}_2)$. Rate limitation by O_2 binding would have the effect of reducing the size of the measured ^{18}O isotope effect for Co-HPAO and introducing a rate reduction with increasing solvent viscosity. As discussed above, the kinetic ^{18}O isotope effect is similar for both forms of the enzyme (Figure 5). Furthermore, solvent viscosogen studies (Figure 4) show an absence of inhibitory effects with WT-HPAO in sucrose and Co-HPAO in glucose. The small effects of glucose with WT-HPAO are tentatively ascribed to reduction of the active site cupric ion by the high concentrations of the reducing sugar in WT-HPAO. While not proven, this suggestion is compatible with the absence of any inhibition of Co-HPAO at similar glucose concentrations. Solvent viscosogen data allow us to eliminate rate limitation of $k_{\text{cat}}/K_m(\text{O}_2)$ by binding of O_2 to the enzyme.

The three-dimensional structure of the anaerobic, reduced form of the *Escherichia coli* CAO was determined recently (4), showing a single water molecule bound to the axial position of the copper ion. Upon addition of oxygen, this water molecule is displaced and peroxide appears close to the axial position of the metal. Loss of the axial water molecule could occur at several points along the mechanism. One possibility is that water is displaced immediately upon O_2 binding to the active site. However, if this were the case in this system, the pK_a for the metal-bound water, seen in $k_{\text{cat}}/K_m(\text{O}_2)$, would not be seen in k_{cat} . As shown above, the pK_a near 7.9, which is attributed to ionization of the metal-

bound water molecule, is seen in both k_{cat} and $k_{\text{cat}}/K_m(\text{O}_2)$ with the wild-type enzyme.

Another point in the mechanism where the metal-bound water molecule could be displaced is concomitant with O_2 reduction and after O_2 binding. With $\text{Cu}^{2+}\text{-OH}$ in the active site, a pre-equilibrium proton transfer from neutral TPQ_{red} to form the anion of TPQ_{red} and $\text{Cu}^{2+}\text{-OH}_2$ would be required prior to electron transfer. This pre-equilibrium proton transfer would not be necessary with $\text{Co}^{2+}\text{-OH}_2$, which is capable of direct displacement by reduced O_2 . Electron transfer from the neutral TPQ_{red} with Co-HPAO would be expected to occur at a significantly slower rate than from the anion of TPQ_{red} with WT-HPAO. Yet, substitution of Co^{2+} for Cu^{2+} in the active site of HPAO does not drastically alter k_{cat} .

Finally, water could be displaced from the metal by superoxide after a rate-limiting electron transfer from TPQ_{red} to O_2 . With $\text{Cu}^{2+}\text{-OH}$ in the active site, proton transfer from the cation form of TPQ_{sq} to metal-bound hydroxide will facilitate loss of water. With $\text{Co}^{2+}\text{-OH}_2$ in the active site, this proton transfer is not necessary. However, since the electron transfer from TPQ_{red} to O_2 is the rate-limiting step in the oxidative half-reaction, mechanistic differences after electron transfer are not expected to be manifest as observable rate differences between the two enzyme forms.

All of the above arguments point toward a dominant, possibly exclusive effect of cobalt substitution on the physical localization of O_2 in the enzyme active site. Previous studies have led to the identification of a nonmetal hydrophobic pocket next to the copper site that is proposed to accommodate bound O_2 (2). By altering the net charge in the active site, ionization of the copper-bound water molecule could have a significant effect on the interaction of O_2 with this site. Copper-bound hydroxide will produce a net charge of +1, as opposed to a net charge of +2 for copper-bound water (Scheme 4). This charge reduction from +2 to +1 cannot be achieved in the physiological pH range with cobalt in the active site and may play a critical role in reducing the affinity of O_2 for Co-HPAO. It could be argued that the increase in charge in Co-HPAO should also have an (opposite?) effect on electron transfer to O_2 to produce the superoxide anion. However, electron transfer from TPQ_{red} to O_2 generates both a positive charge on the resulting TPQ_{sq}⁺ and a negative charge on $\text{O}_2^{\bullet-}$, leaving their combined charge neutral. Thus, the net charge at the active site is expected to

remain unchanged during the rate-limiting electron transfer step, pointing toward the primary effect of the increased charge in Co-HPAO on the preceding, O₂ binding step.

Concluding Comments. As introduced above, all experimental parameters point toward highly similar mechanisms for the reaction of molecular oxygen with the copper and cobalt forms of reduced HPAO. It is particularly intriguing how cobalt substitution can leave the mechanism for O₂ reduction unaltered, while reducing $k_{\text{cat}}/K_{\text{m}}(\text{O}_2)$ by several orders of magnitude. Probably the most important observation in this context is the elevated $\text{p}K_{\text{a}}$ for cobalt-bound water. As shown in Scheme 4, ionization of one of the copper-bound water molecules reduces the net charge at the metal center from +2 to +1. Since the metal site is directly adjacent to the proposed hydrophobic binding pocket for O₂ (2), the overall charge is expected to play an important, hitherto unrecognized, role in O₂ affinity. We propose that the failure of the cobalt-bound water molecule to ionize in the physiological pH range produces a net increase of +1 on the charge experienced by bound O₂ in Co-HPAO. This has its major effect on a decreased affinity of O₂ for its site, providing an explanation for the very significant decrease in $k_{\text{cat}}/K_{\text{m}}(\text{O}_2)$ for Co-HPAO in relation to that of WT-HPAO while leaving k_{cat} largely unaltered.

REFERENCES

1. Medda, R., Padiglia, A., Bellelli, A., Pedersen, J. Z., Agro, A. F., and Floris, G. (1999) *FEBS Lett.* 453, 1–5.
2. Su, Q., and Klinman, J. P. (1998) *Biochemistry* 37, 12513–12525.
3. Turowski, P. N., McGuirl, M. A., and Dooley, D. M. (1993) *J. Biol. Chem.* 268, 17680–17682.
4. Wilmot, C. M., Hajdu, J., McPherson, M. J., Knowles, P. F., and Phillips, S. E. V. (1999) *Science* 286, 1724–1728.
5. Dooley, D. M., McGuirl, M. A., Brown, D. E., Turowski, P. N., McIntire, W., and Knowles, P. F. (1991) *Nature* 349, 262–264.
6. Mills, S. A., and Klinman, J. P. (2000) *J. Am. Chem. Soc.* 122, 9897–9904.
7. Drummond, J. T., and Matthews, R. G. (1994) *Biochemistry* 33, 3732–3741.
8. Plastino, J., Green, E. L., Sanders-Loehr, J., and Klinman, J. P. (1999) *Biochemistry* 38, 8204–8216.
9. Cai, D., and Klinman, J. P. (1994) *Biochemistry* 33, 7647–7653.
10. Cai, D., and Klinman, J. P. (1994) *J. Biol. Chem.* 269, 23039–23042.
11. Hevel, J. M., Mills, S. A., and Klinman, J. P. (1999) *Biochemistry* 38, 3683–3693.
12. Cleland, W. W. (1979) *Methods Enzymol.* 63, 103–138.
13. Schowen, B. K., and Schowen, R. L. (1982) *Methods Enzymol.* 87, 551–606.
14. Su, Q., and Klinman, J. P. (1999) *Biochemistry* 38, 8572–8581.
15. Tian, G., Berry, J. A., and Klinman, J. P. (1994) *Biochemistry* 33, 226–234.
16. Mure, M., and Klinman, J. P. (1993) *J. Am. Chem. Soc.* 115, 7117–7127.
17. Agostinelli, E., De Matteis, G., Mondovi, B., and Morpurgo, L. (1998) *Biochem. J.* 330, 383–387.
18. De Matteis, G., Agostinelli, E., Mondovi, B., and Morpurgo, L. (1999) *J. Biol. Inorg. Chem.* 4, 348–353.
19. Richens, D. T. (1997) *The Chemistry of Aqua Ions*, John Wiley & Sons, New York.
20. Francisco, W., Tian, G., Fitzpatrick, P. F., and Klinman, J. P. (1998) *J. Am. Chem. Soc.* 120, 4057–4062.
21. Su, Q. (1998) Ph.D. Dissertation, University of California, Berkeley, CA.

BI0200864